JOURNAL OF MATERIALS SCIENCE 26 (1991) 2137–2142

Texture development in uniaxially drawn polyethylene tape

N. S. J. A. GERRITS
Department of Materials Technology, DSM Research, P.O. Box 18, 6160 MD Geleen, The Netherlands

R. J. YOUNG
Polymer Science and Technology Group, Manchester Materials Science Centre, UMIST, P.O. Box 88, Manchester, M60 1QD, UK

Texture development in solid-state uniaxially drawn polyethylene has been interpreted in terms of crystal plasticity and deformation in the amorphous phase. A poorly defined texture with the chain axes normal to the sample surface develops at low draw ratios ($\lambda = 2$). The development of this texture is explained by interlamellar shear taking place in the amorphous phase. On further drawing, the chain axes rotate parallel to the draw direction. This rotation is governed by (duplex) slip on several systems such as (1 0 0) [0 1 0] and $\{1\,1\,0\}\langle 1\bar{1}\,0\rangle$ transverse slip and (1 0 0) [0 0 1], (0 1 0) [0 0 1] and $\{1\,1\,0\}\langle 0\,0\,1\rangle$ chain slip. At higher draw ratios ($\lambda \geqslant 11$) the chain axis is parallel to the draw direction and (1 0 0) planes become parallel to the sample surface. This orientation, often called a (1 0 0) texture, cannot necessarily be related to single slip on (1 0 0) planes. The texture could also be generated by cross slip on (1 0 0) [0 0 1] and $\{1\,1\,0\}\langle 0\,0\,1\rangle$ slip systems. It is postulated that any type of slip on (0 1 0) planes is restricted due to fold plane restraints.

1. Introduction

Over the past 30 years there have been several detailed studies of the solid-state drawing of polyethylene [1–6]. It is clear that during uniaxial deformation there is a discontinuous transformation from the original isotropic material into deformed specimens which have their polymer chains oriented parallel to the draw direction but the exact nature of this deformation process is still not fully understood. For example, before full chain orientation occurs, intermediate textures can develop. Also "local melting" has been invoked by some authors [7, 8] to explain the close relationship between the long period and drawing temperature, although others dispute this suggestion [6].

In this paper we attempt to describe the deformation process from considerations of crystal plasticity following the approach of Bowden and Young [9]. The particular aspects considered are the dislocation energy, and the critical resolved shear stress and the fold plane restraints during the activation of particular slip systems. The possibilities of duplex slip and cross slip occurring within a polyethylene crystal have been considered. Furthermore the relationship between the texture development and operating slip systems is analysed. Normal uniaxial drawing produces specimens with a fibre texture which does not provide a good insight into the deformation processes. Because of this, constrained uniaxial drawing of solution-crystallized ultra-high molecular weight polyethylene (UHMW-PE) films has been employed. Such materials can be deformed to high draw ratios but are also found to have three-dimensional crystallite orientation which is analogous to rolled or compression-drawn material studied by previous workers [1, 4, 9].

2. Crystal deformation and texture development

2.1. Slip systems

Several methods can be used to predict the slip systems that will operate when a force is applied to a polymer crystal. The simplest method is to assume that slip will take place preferentially on the closest packed planes in the closest packed directions as is found with metal crystals. However, because the bonding in polymer crystals is highly anisotropic, such a simple analysis is not of general use.

A more sophisticated approach is to use dislocation theory [10–13] whereby the energy required for a specific slip system to operate can be calculated. Shadrake and Guiu [12] and Bacon and Tharmalingam [13] calculated the energy required for the operation of different slip systems during the deformation of polyethylene at room temperature. It is found from considerations of dislocation energy that chain slip on $\{hk0\}$ planes is more favourable than transverse slip. On the other hand, it is found that if transverse slip does take place then the (1 0 0) [0 1 0] slip system has the lowest dislocation energy. However, the dislocation energy of the $\{1\,1\,0\}\langle 1\bar{1}\,0\rangle$ slip systems can be

0022–2461/91 $03.00 + .12

reduced by dissociation of the dislocations into partials [12, 13]. Also it has been postulated that a fold plane structure will impose restraints upon the operation of slip systems during transverse slip [10, 12, 14]. Because only {1 1 0} or (1 0 0) fold planes are found in polyethylene [15, 16] it would appear that from both fold plane restraints and dislocation energetics, (0 1 0) [1 0 0] transverse slip is unlikely to operate in polyethylene. An extra complication for the deformation of polyethylene is the operation of an orthorhombic–monoclinic phase transformation and {3 1 0} and {1 1 0} twinning processes [1, 2, 9, 14, 17–19] during deformation perpendicular to the chain axes.

It is known that for a polycrystalline material undergoing general deformation, *five* independent slip systems are needed to compensate for *any* arbitrary strain (see Kelly and Groves [20]). However, due to the restrictions upon breaking covalent bonds, only four *independent* slip systems, (1 0 0) [0 0 1], (1 1 0) [0 0 1], (1 0 0) [0 1 0] and (1 1 0) [1 $\bar{1}$ 0], are available in orthorhombic polyethylene. All of the other chain slip and transverse slip systems can be made from combinations of these four. There is no doubt that polyethylene can undergo high degrees of plastic deformation at room temperature for any arbitrary strain. This must be due to deformation within the rubbery amorphous regions allowing the accommodation of crystal shape changes without cracking [9].

2.2. Resolved shear stress criterion

The considerations outlined above give only an indication of the slip systems able to operate in a semi-crystalline polymer from considerations of the energies involved. When a polymer crystal is subjected to a general deformation then the operations of particular slip systems will depend upon the geometry of the deformations, in particular the relationship between the direction of the applied force and the slip systems. This can be analysed in terms of the resolved shear stress criterion which is applied extensively to the deformation of metal crystals but has also been shown by Bowden and Young [4, 21, 22] to be useful in the analysis of yield in polymer crystals. The resolved shear stress on the slip plane in the slip directions is given by

$$\tau = \sigma \cos \phi_0 \cos \lambda_0 \qquad (1)$$

where σ is the tensile or compressive stress parallel to the applied force (F), λ_0 is the angle between F and the slip direction and ϕ_0 is the angle between F and the normal to the slip plane [23]. The resolved shear stress on any slip system can be evaluated from Equation 1. When several slip systems are available for the deformation of a crystal a convenient way of deciding which one is subjected to the largest resolved shear stress (and hence is operative) is to use a stereographic projection [23]. Fig. 1 shows the effective slip systems in orthorhombic polyethylene. The main advantage of using a stereographic projection is that the angles between an arbitrary applied force and the slip direction (λ_0) and between this force and the normal to the slip plane (ϕ_0) can be readily determined.

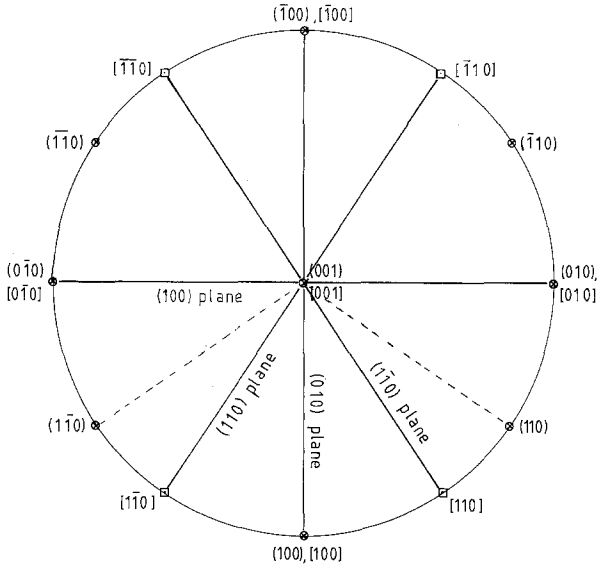

Figure 1 Stereographic projection of the orthorhombic unit cell of polyethylene. The energetically favourable slip planes are given in relation to possible slip directions.

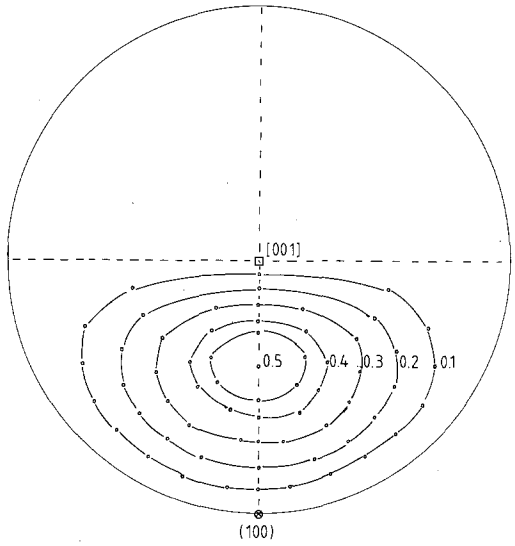

Figure 2 Stereographic projection of the (1 0 0) [0 0 1] slip system with the Schmid factor (cos ϕ_0 cos λ_0) given for any orientation of the tensile axis.

In Fig. 2 contours are drawn on the 0 0 1 stereographic projection joining directions of loading which have equal values of the Schmid factor (cos ϕ_0 cos λ_0) for the (1 0 0) [0 0 1] slip system. The values of the Schmid factor vary between 0 and 0.5 and reach the maximum when $\phi_0 = \lambda_0 = 45°$. It can be seen from Fig. 2 that the highest value of resolved shear stress for the (1 0 0) [0 0 1] slip system is when a force F, is applied approximately parallel to the [1 0 3] direction.

Fig. 3 shows the variation of Schmid factor with loading direction when all the three (1 0 0) [0 0 1], and (0 1 0) [0 0 1] and {1 1 0} ⟨0 0 1⟩ slip systems operate. These slip systems are known to have similar deformation energies [12, 13]. It can be seen that the Schmid factor is very similar for all directions possessing an angle of 45° to [0 0 1] with one maximum of 0.5 in each of the eight sectors in the stereogram.

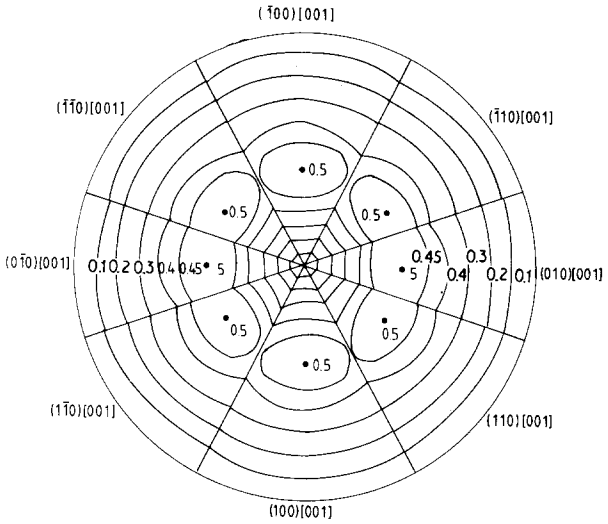

Figure 3 Stereographic projection with the Schmid factor given for chain slip on the (1 0 0) [0 0 1], (0 1 0) [0 0 1] and {1 1 0} ⟨0 0 1⟩ slip systems.

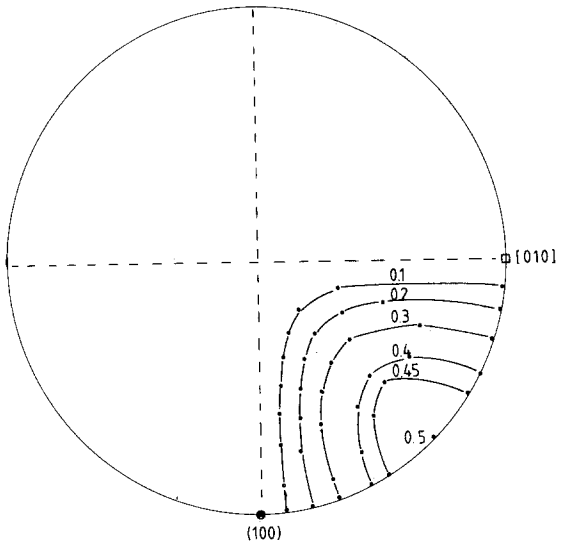

Figure 4 Stereographic projection with the Schmid factor given for transverse slip on the (1 0 0) [0 1 0] slip system.

Figs 4 and 5 show the variation of Schmid factor with the direction of applied force for both the single (1 0 0) [0 1 0] slip system and the combination of (1 0 0) [0 1 0] and {1 1 0} ⟨1 1̄ 0⟩ slip systems, respectively. It can be seen from Fig. 5 that the resolved shear stress for transverse slip is greatest for forces applied perpendicular to the chain axes with several maxima of 0.5 around the perimeter of the stereogram.

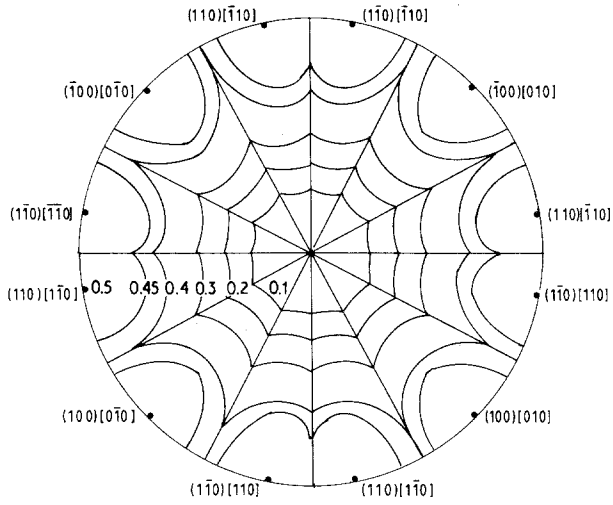

Figure 5 Stereographic projection with the Schmid factor given for transverse slip on both the (1 0 0) [0 1 0] and {1 1 0} ⟨1 1̄ 0⟩ slip systems.

2.3. Texture development

During the deformation of a polycrystalline material a texture may develop whereby certain crystallographic planes and directions become preferentially oriented relative to compression or tensile axes. If deformation takes place through the operation of one slip system (*single slip*) then the situation can be readily analysed. In this case the slip direction approaches the tensile axis and the normal to the slip plane approaches the compression direction [20].

In most crystal structures, however, there is a multiplicity of potential slip systems. Under certain loading conditions two of these systems may experience similar stresses, and when the yield criterion is satisfied, slip may occur on both systems simultaneously. This type of deformation is termed *duplex slip* which can refer to two slip directions on a common slip plane or two slip planes with a common slip direction [23]. If duplex slip occurs, it can be shown that in tension crystals rotate towards the vector sum of both slip directions and in compression towards the vector sum of the normals to the slip plane [23].

In the case where two or more slip planes share a common slip direction it is possible for a moving dislocation to change from one slip plane to another through a process known as *cross slip*. The process occurs only with screw dislocations [20] which are the lowest energy type of dislocations in polyethylene [12, 13]. Cross slip can result in a wavy single crystal texture, for example in polyethylene, simultaneous slip on (1 0 0), (1 1 0) and (1 1̄ 0) planes in the [0 0 1] direction can give rise to a (1 0 0) texture. This is illustrated schematically in Fig. 6. It should be noted that cross slip may reduce significantly the shear stresses required for slip due to the availability of a large number of slip planes [20].

The above considerations are concerned only with the geometry of slip. The activation of a particular slip system will depend on both the geometry of deformation and the deformation energy for slip. For example, in polyethylene both chain slip and transverse slip can be geometrically equally favourable. However, the dislocation energies for chain slip are considerably lower [12, 13] than for transverse slip and this results in a chain axis orientation parallel to the tensile axis at large deformations.

3. Experimental procedure

3.1. Sample preparation

Solution-crystallized UHMW-PE films were prepared by continuously extruding a 15% solution of UHMW-PE (Himont HB312 CM, $M_w = 1.5$

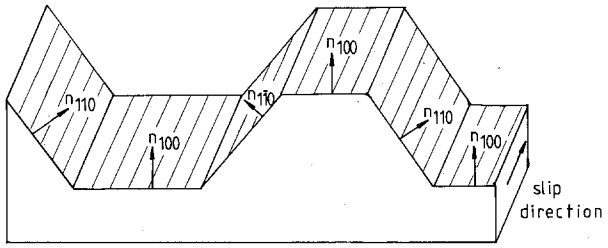

Figure 6 Schematic representation of cross slip on (1 0 0) and {1 1 0} planes in the [0 0 1] direction and development of a (1 0 0) texture.

$\times 10^3$ kg mol^{-1}) in decalin. The solution was quenched in water and the resultant film was dried at ambient temperature to a concentration of 80% UHMW-PE in decalin.

The films were drawn uniaxially constrained at constant width using a stretching frame made by Iwamoto Seisakusho Ltd. The initial sample dimensions were 60 × 60 mm^2 and a cross head speed of 20 mm s^{-1} and a temperature of 120 °C were employed for the drawing process. The exact draw ratios ranging between 1 and 20 were determined by measuring the displacement of ink marks, placed 1 cm apart onto the specimen prior to drawing. Draw ratios below 10 could be achieved in a single-step drawing process, whereas for draw ratios above 10 a two-step drawing process was used due to limitations of the stretching frame.

3.2. Wide-angle X-ray diffraction

To determine the crystal orientation, wide-angle X-ray scattering (WAXS) patterns were obtained by a Statton camera with a flat-film geometry and Ni-filtered Cu$K\alpha$ radiation from a Philips PW1729 generator operated at 50 kV and 40 mA was employed. Photographs were recorded at room temperature with the incident X-ray beam both normal and parallel to the sample surface.

Texture measurements were carried out on a computer-controlled Siemens diffractometer, which incorporated a Huber Eulerian cradle model 511.4. The intensity of the X-rays reflected from the (1 1 0) and (2 0 0) lattice planes was measured as function of the three dimensional positioning of the sample by varying the χ and ϕ angles on the Eulerian circle. The texture measurements were carried out using a STOE rotating anode (7 kW, Ni-filtered CuKα radiation). The angle χ between sample normal and measuring plane was scanned in steps of 5°. A continuous count procedure was used to collect data in 5° ϕ intervals for the full range of 0–360° (ϕ is the angle of rotation around the sample normal.) A complete pole figure is determined by combining a reflection (χ = 0–65°) and a transmission measurement (χ = 65–90°).

The pole figures were calculated from the experimental data by commercial Siemens TEX11 software. The measured data were corrected for background radiation by subtracting a value obtained from linear interpolation of values measured at both low and high 2θ positions. The theoretical variation of the intensity was calculated as a function of both the χ and ϕ angles and the sample thickness times absorption coefficient. A texture-free sample of polyethylene was used for correcting the defocusing effect. The measured reflection and transmission data were combined using a set of intensities with common χ = 65°. After the preceding corrections, the intensities were normalized with regard to the unit of a random intensity and the pole figures were plotted.

3.3. Small-angle X-ray diffraction

Small-angle X-ray scattering (SAXS) patterns were determined using a Kiessig camera equipped with a very fine pinhole collimation system. Ni-filtered CuKα radiation generated at 50 kV and 40 mA from a Philips PW1730 generator was employed. The sample-to-film distance was 400 mm and photographs were recorded with the incident X-ray beam both normal and parallel to the sample surface.

4. Results

Fig. 7 shows WAXS and SAXS patterns recorded with the X-ray beam both normal and parallel to the sample surface over a range of different draw ratios from λ = 1–20. At small draw ratios ($\lambda \leqslant 2$) the original isotropic crystal orientation is transformed into a structure where lamellae become oriented with their normals preferentially perpendicular to the sample surface, as can be seen from the SAXS pattern in Fig. 7d for λ = 2. This is accompanied by the development of a poorly defined texture in which the chain axes become normal to the draw direction (Fig. 7c). At λ = 3 two types of crystal orientation can be observed from both the WAXS and the SAXS pattern recorded with the beam parallel to the tape (Fig. 7c and d). One set of crystals has a similar orientation as for λ = 2, whereas the other set show the development of a chain axis orientation parallel to the draw direction. Between draw ratios of 5 and 11 the crystal orientation becomes more uniform as shown by the gradual sharpening of the arcs in the WAXS patterns and the development of a second order reflection in the SAXS patterns (Fig. 7b and d). For $\lambda \geqslant 11$ a (1 0 0) texture develops as illustrated by the (2 0 0) reflection having a higher intensity than the (1 1 0) reflection in the WAXS pattern in Fig. 7c (λ = 20). The development of this texture is accompanied by an increase in the long period measured by SAXS.

It should be noted that the (1 0 0) texture is not particularly well-defined and (1 1 0) reflections are also observed when the X-ray beam is aligned parallel to the sample surface (Fig. 7c). This weak {1 1 0} texture could be the result of a large orientation distribution in a plane perpendicular to the drawing direction or processes such as {3 1 0} or {1 1 0} twinning.

To distinguish between these two possible explanations, pole figures of both the (1 1 0) and (2 0 0) reflections were recorded for a highly drawn sample (λ = 16). It is shown by the pole figures in Fig. 8 that

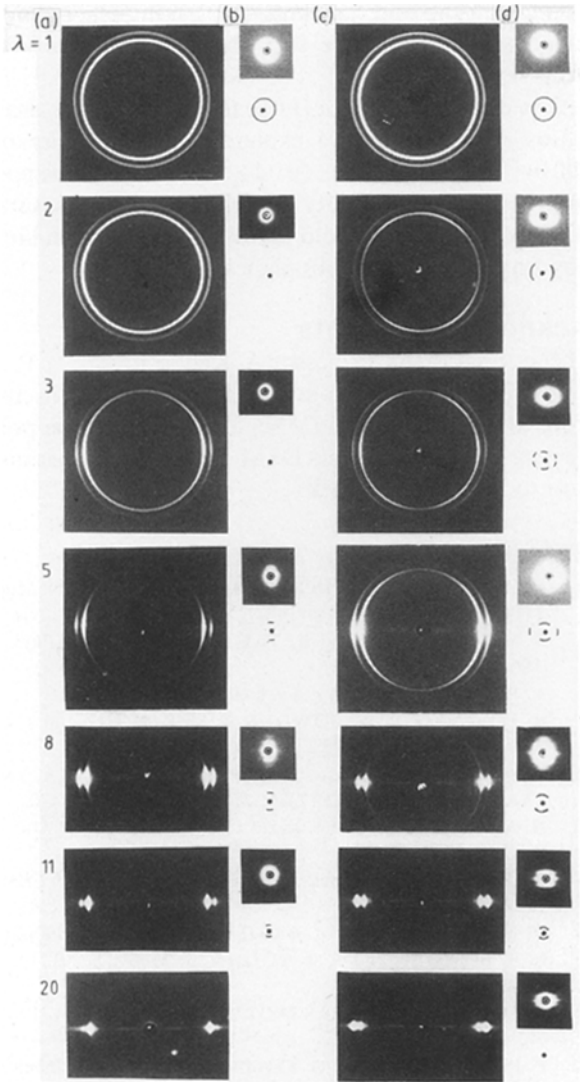

Figure 7 WAXS and SAXS patterns of uniaxially drawn polyethylene tape recorded with the incident X-ray beam (a, b) normal and (c, d) parallel to the sample surface. The draw direction is vertical and the draw ratio is indicated in each case.

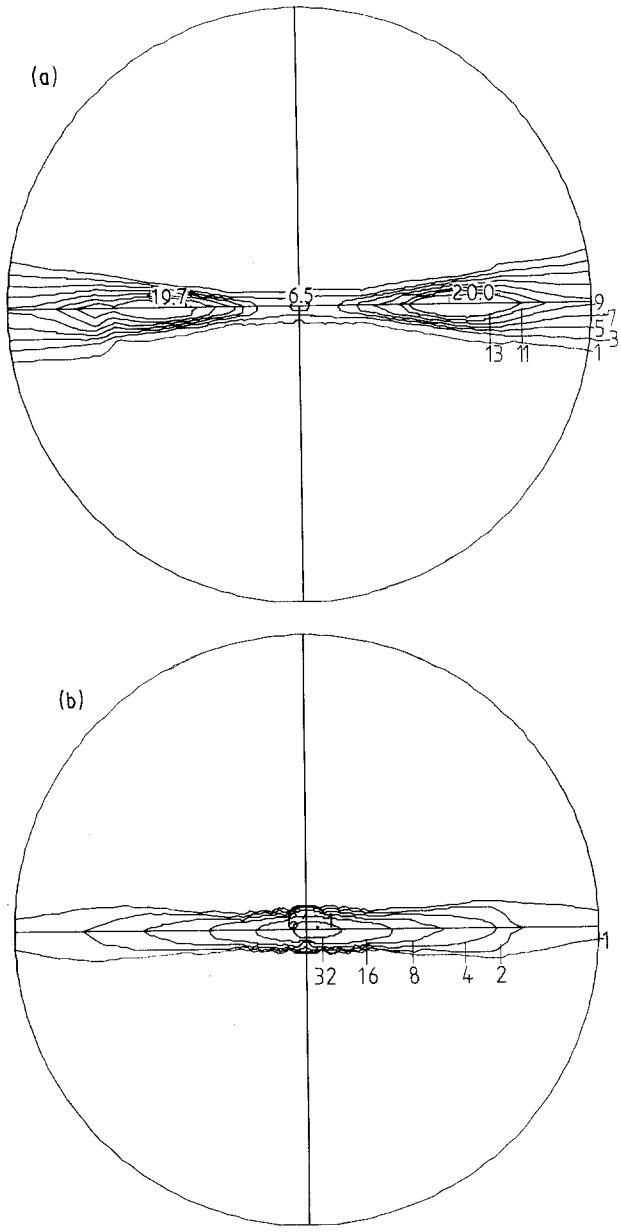

Figure 8 Pole figures of a polyethylene tape drawn up to a draw ratio of 16. The draw direction is vertical and the direction normal to the sample surface is located in the middle of the pole figure. Contour levels are indicated. (a) (1 1 0) reflection, (b) (2 0 0) reflection.

the sample possesses a (1 0 0) texture which is not very well defined. However, a relatively low (1 1 0) intensity maximum is observed in the centre of the (1 1 0) pole figure (Fig. 8a) indicating a small amount of (1 1 0) texture.

5. Discussion

It can be concluded from the X-ray diffraction patterns in Fig. 7 that the original material ($\lambda = 1$) has an isotropic crystal orientation. In the initial stages of drawing this structure is transformed into a structure where lamellae normals become perpendicular to the sample surface and the crystal *c*-axes normal to the draw direction. This transformation can be only explained by a non-crystallographic deformation mechanism such as interlamellar slip, due to deformation in the amorphous phase [4]. This deformation mechanism is shown schematically in Fig. 9 and this form of lamella rotation has been considered by Peterlin [3] to explain the development of texture during the uniaxial drawing of melt-crystallized polyethylene.

On further drawing, tensile forces will be applied approximately normal to the crystallographic *c*-axes. On the basis of the critical resolved shear stress this is a favourable orientation for transverse slip to take place (Fig. 5). Because our samples are thought to possess a mixed $\{1\,1\,0\}$ and (1 0 0) fold plane structure, the $\{1\,1\,0\}\ \langle 1\,\bar{1}\,0\rangle$ and (1 0 0) [0 1 0] transverse slip systems will be equally likely to occur. As the texture at $\lambda = 2$ is not well defined and dislocation energy for chain slip is lower than for transverse slip, the $\{1\,1\,0\}$ and (1 0 0) slip planes can also accommodate chain slip in the [0 0 1] direction. Furthermore, it is likely that in a sample with a spread of crystal orientation, duplex slip will occur by combination of chain slip and transverse slip on the same plane. The particular slip systems operating in an individual crystal will depend on the exact crystal orientation and the fold plane structure. This deformation, which will take place

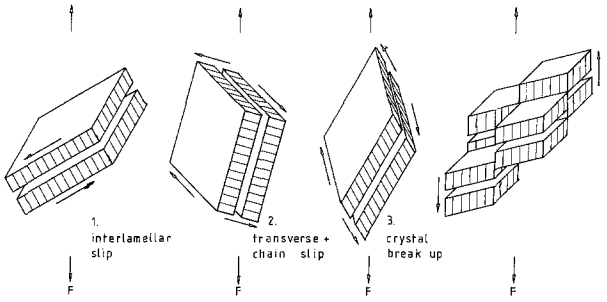

Figure 9 Schematic representation of crystal deformation in uniaxially drawn polyethylene between a draw ratio of 1 and 5. The following stages can be distinguished; (1) interlamellar shear, (2) transverse slip and chain slip (affine slip), and (3) crystal break up by chain slip (coarse slip).

initially in an *affine* manner [9], is shown schematically in Fig. 9.

The activation of these deformation processes will result in the rotation of the chain axes and the long period relative to the tensile axis. This process is accompanied by a crystal break up, as has been shown clearly by apparent crystallite size (ACS) measurements reported by van Aerle and Braam [6]. The process of crystal break up is completely consistent with *coarse* slip taking place on localized slip planes in the later stages of deformation [9].

At higher strains ($\lambda \geqslant 11$) a well-defined texture develops such that the chain axis become parallel to the draw direction and the (1 0 0) planes oriented parallel to the sample surface (Fig. 8). This type of (1 0 0) texture has been observed in uniaxial deformation of both melt-crystallized [24–26] and solution-crystallized polyethylene [5, 6, 27]. It has been interpreted as being due to the principal slip plane in polyethylene being (1 0 0) [5, 25, 27]. But, as was shown in a former paragraph, a (1 0 0) texture can be generated by either single slip or cross slip on planes which are a combination of (1 1 0), (1 $\bar{1}$ 0) and (1 0 0) planes. If slip could also take place on (0 1 0) planes, a fibre texture would develop on constrained uniaxial drawing of polyethylene. It therefore appears that the absence of (0 1 0) fold planes and the consequent restriction of the (0 1 0) [1 0 0] transverse slip process restrict any type of slip on (0 1 0) planes. It is also likely that the fold plane restrictions will make deformation by *coarse* (0 1 0) [0 0 1] chain slip more difficult.

6. Conclusions

The constrained uniaxial deformation of polyethylene in the solid-state has been described in terms of crystal plasticity. The initial isotropic lamellar orientation is transformed by interlamellar shear into an orientation of the lamellae with their normals perpendicular to the sample surface. When $\lambda = 2$ the chain axes are oriented approximately normal to the draw direction and consequently *transverse slip* on both $\{1\,1\,0\}\ \langle 1\,\bar{1}\,0\rangle$ and (1 0 0) [0 1 0] slip systems is expected to operate. The texture is poorly defined and for crystals with chain directions not normal to the draw direction deformation can proceed by *chain slip* on (1 0 0) [0 0 1] and $\{1\,1\,0\}\ \langle 0\,0\,1\rangle$ slip systems. *Duplex slip* due to both chain slip and transverse slip taking place simultaneously on the same slip plane, is also likely to occur.

The development of a (1 0 0) texture at higher draw ratios ($\lambda \geqslant 11$) may be explained by *cross slip* on (1 0 0) [0 0 1] and $\{1\,1\,0\}\ \langle 0\,0\,1\rangle$ slip systems. It is postulated that the inability of (0 1 0) [1 0 0] transverse slip to occur is due to fold plane restraints which limit any type of slip on (0 1 0) planes.

Acknowledgements

The authors thank Professor A. Keller, Professor P. J. Lemstra and Dr W. Pontenagel for valuable discussions and C. van Halen (MSc) for producing the pole figures. They also thank DSM Research for permission to publish this work.

References

1. F. C. FRANK, A. KELLER and A. O'CONNOR, *Phil. Mag.* **3** (1958) 64.
2. T. SETO, T. HARA and K. TANAKA, *Jpn J. Appl. Phys.* **7** (1968) 31.
3. A. PETERLIN, *J. Mater. Sci.* **6** (1971) 490.
4. R. J. YOUNG, P. W. BOWDEN, J. M. RITCHIE and J. G. RIDER, *ibid.* **8** (1973) 23.
5. T. KANAMOTO, A. TSURUTA, K. TANAKA, M. TAKEDA and R. S. PORTER, *Macromol.* **21** (1988) 470.
6. N. A. J. M. VAN AERLE and A. W. M. BRAAM, *J. Mater. Sci.* **23** (1988) 4429.
7. R. CORNELIUSSEN and A. PETERLIN, *Makromol. Chem.* **105** (1967) 193.
8. D. M. SADLER and P. J. BARHAM, *Polymer* **31** (1990) 36.
9. P. B. BOWDEN and R. J. YOUNG, *J. Mater. Sci.* **9** (1974) 2034.
10. H. D. KEITH and E. PASSAGLIA, *J. Res. NBS* **68A** (1964) 513.
11. P. PREDECKI and W. O. STATTON, *Appl. Polym. Symp.* **6** (1967) 165.
12. L. G. SHADRAKE and F. GUIU, *Phil. Mag.* **34** (1976) 565.
13. D. J. BACON and K. THARMALINGAM, *J. Mater. Sci.* **18** (1983) 884.
14. P. ALLAN and M. BEVIS, *Proc. R. Soc. London* **A341** (1974) 75.
15. XIABIN JING and S. KRIMM, *J. Polym. Sci. Polym. Phys. Ed.* **20** (1982) 1155.
16. S. J. SPELLS, S. J. ORGAN, A. KELLER and G. ZERBI, *Polymer* **28** (1987) 697.
17. H. KIHO, A. PETERLIN and P. H. GEIL, *J. Appl. Phys.* **5** (1964) 1599.
18. R. J. YOUNG and P. B. BOWDEN, *Phil. Mag.* **29** (1974) 1061.
19. P. ALLAN and M. BEVIS, *ibid.* **41** (1980) 555.
20. A. KELLY and G. W. GROVES, "Crystallography of Crystal Defects" (Longman, London, 1970).
21. P. B. BOWDEN and R. J. YOUNG, *Nature Phys. Sci.* **229** (1971) 23.
22. R. J. YOUNG, *Mater. Forum* **11** (1988) 210.
23. N. REID, "Deformation Geometry for Materials Scientists", International series on materials science and technology, Vol. 11, edited by W. S. Owen (Pergamon Press, 1973).
24. J. J. POINT, G. A. HOMÉS, D. GEZOVICH and A. KELLER, *J. Mater. Sci.* **4** (1969) 908.
25. O. YODA and I. KURIYAMA, *J. Polym. Sci. Polym. Phys. Ed.* **15** (1977) 773.
26. A. KAITO, K. NAKAYAMA and H. KANETSUNA, *J. Appl. Polym. Sci.* **30** (1985) 1241.
27. K. ISHIKAWA, K. MIYASAKA and M. MAEDA, *J. Polym. Sci. A-2* **7** (1969) 2029.

Received 10 October 1989
and accepted 24 April 1990